Inorg. Chem. **2003**, *42*, 2538–2544

Polymorphism of Heptalithium Nitridovanadate(V) $Li_7[VN_4]$

R. Niewa,*,† D. Zherebtsov,† and Z. Hu‡

Max-Planck-Institut für Chemische Physik fester Stoffe, Nöthnitzer Str. 40, D-01187 Dresden, Germany, and II. Physikalisches Institut der Universität zu Köln, Zülpicher Str. 77, D-50937 Köln, Germany

Received November 4, 2002

The system Li–V–N was studied by means of X-ray and neutron powder diffraction, thermal and chemical analyses, and XAS spectroscopy at the vanadium K-edge. Three polymorphs of $Li_7[VN_4]$ have been established from X-ray and neutron powder diffraction (γ-$Li_7[VN_4]$, space group $P\bar{4}3n$, No. 218, $a = 960.90(4)$ pm, $V = 887.23(6) \times 10^6$ pm^3, $Z = 8$; β-$Li_7[VN_4]$, space group $Pa\bar{3}$, No. 205, $a = 959.48(3)$ pm, $V = 883.31(5) \times 10^6$ pm^3, $Z = 8$; α-$Li_7[VN_4]$, $P4_2/nmc$, No. 137, $a = 675.90(2)$ pm, $c = 488.34(2)$ pm, $V = 223.09(1) \times 10^6$ pm^3, $Z = 2$). Crystallographic and phase relations are discussed. All three modifications are diamagnetic, indicating vanadium in the oxidation state +5. The V–K XAS spectra support the oxidation state assignment, the non-centrosymmetric coordination (tetrahedral), and the nearly identical second coordination sphere of vanadium, made up from Li in all three phases. The 3d-related features of the spectra display strongly localized properties. The phase transitions appear to be reconstructive; no direct group–subgroup symmetry relations of the crystal structures exist. The formation of solid solutions between Li_2O and β-$Li_7[VN_4]$ with the general formula $Li_{1.75}\{(V_{0.25(1-x)}Li_{0.25x})(N_{1-x}O_x)\}$ with $0 \leq x \leq 1$ leads to increasing substitution of V by Li. At the approximate composition with $x = 0.125$ the Li–V-disorder seems to be complete: X-ray diffraction lines give rise to only one-half of the original unit cell dimensions, $a' = 476.47(3)$ pm $\approx (1/2)a(\beta\text{-}Li_7[VN_4])$.

Introduction

Lithium nitridometalates of the transition metals have been studied intensively since the early pioneering work of Robert Juza et al.[1–4] In the row of the 3d transition metal compounds one can find a preference of the unusual low oxidation state +1 for Cu, Ni, and Co.[5] These elements form with Li_3N in nitrogen atmosphere solid solution series $Li_2[(Li_{1-x}M^I_x)N]$ with the α-$Li_3N \equiv Li_2[LiN]$ structure type in a broad range of compositions. For the group 8 metal Fe the most stable compound is $Li_3[Fe^{III}N_2]$[6] with iron in the oxidation state +3. Yet, thermal decomposition in the absence of molecular nitrogen leads to $Li_4[Fe^{II}N_2]$[7] and $Li_2[(Li_{1-x}Fe^I_x)N]$.[8] The latter phase shows unusual magnetic properties and the highest hyperfine field ever observed in Mössbauer studies for an iron compound.[9] The situation in the case of the nitridomanganates is similar: $Li_7[Mn^VN_4]$ is obtained from manganese and excess Li_3N in nitrogen atmosphere.[10] This compound can be decomposed in argon atmosphere successively to $Li_{24}[Mn^{III}N_3]_3N_2$, $Li_5[(Li_{1-x}Mn^{+1.6}_x)N]_3$, and $Li_2[(Li_{1-x}Mn^I_x)N]$, to finally yield the binary manganese nitrides Mn_2N and Mn_4N.[11,12] A nitridomanganate(VII) is not known so far.[13] For Cr, V, and Ti only ternary lithium nitridometalates with the highest oxidation states of the transition metals were reported: $Li_6[Cr^{VI}N_4]$,[14] $Li_{15}[Cr^{VI}N_4]_2N$,[14] $Li_7[V^VN_4]$,[15,16] and $Li_5Ti^{IV}N_3$.[17] All crystal structures of these

* Author to whom correspondence should be addressed. E-mail: niewa@cpfs.mpg.de.
† Max-Planck-Institut für Chemische Physik fester Stoffe.
‡ II. Physikalisches Institut der Universität.

(1) Juza, R.; Langer, K.; von Benda, K. *Angew. Chem.* **1986**, *80*, 373.
(2) Niewa, R.; Jacobs, H. *Chem. Rev.* **1996**, *96*, 2053.
(3) Kniep, R. *Pure Appl. Chem.* **1997**, *69*, 185.
(4) Niewa, R.; DiSalvo, F. J. *Chem. Mater.* **1998**, *10*, 2733.
(5) Sachsze, W.; Juza, R. *Z. Anorg. Allg. Chem.* **1949**, *259*, 278.
(6) Gudat, A.; Kniep, R.; Rabenau, A.; Bronger, W.; Ruschewitz, U. *J. Less-Common Met.* **1990**, *161*, 31.
(7) Gudat, A.; Kniep, R.; Rabenau, A. *Angew. Chem.* **1991**, *103*, 217.
(8) Klatyk, J.; Kniep, R. *Z. Kristallogr. NCS* **1999**, *214*, 447.
(9) Klatyk, J.; Schnelle, W.; Wagner, F. R.; Niewa, R.; Novák, P.; Kniep, R.; Waldeck, M.; Ksenofontov, V.; Gütlich, P. *Phys. Rev. Lett.* **2002**, *88*, 207202.
(10) Juza, R.; Anschütz, E.; Puff, H. *Angew. Chem.* **1959**, *71*, 161.
(11) Klatyk, J.; Kniep, R. *Z. Kristallogr. NCS* **1999**, *214*, 445.
(12) Niewa, R.; Wagner, F. R.; Schnelle, W.; Hochrein, O.; Kniep, R. *Inorg. Chem.* **2001**, *40*, 5215.
(13) Niewa, R. *Z. Kristallogr.* **2002**, *217*, 8.
(14) Gudat, A.; Haag, S.; Kniep, R.; Rabenau, A. *Z. Naturforsch. B* **1990**, *45*, 111.
(15) Juza, R.; Gieren, W.; Haug, J. *Z. Anorg. Allg. Chem.* **1959**, *300*, 61.
(16) Niewa, R.; Kniep, R. *Z. Kristallogr. NCS* **2001**, *216*, 5.

10.1021/ic020653b CCC: $25.00
Published on Web 03/26/2003

lithium nitridometalates with the 3d transition metal in the highest oxidation states can be described as superstructures of the Li_2O type.

Initially, $Li_7[VN_4]$ was prepared at temperatures below 1020 K and described in the cubic space group $P\bar{4}3n$ with 8 formula units in the unit cell.[15] This ordered $2 \times 2 \times 2$ Li_2O superstructure is one possible example of eight isolated tetrahedra $[VN_4]^{7-}$ within a face centered cubic (fcc) arrangement of nitride ions. Interestingly, $Li_7[MnN_4]$[10] and $Li_7[PN_4]$[17] are isotypes ($P\bar{4}3n$), while $Li_7[NbN_4]$[18] and $Li_7[TaN_4]$[19] are reported to crystallize with the cubic space group $Pa\bar{3}$, also with 8 formula units per unit cell. For some time we have observed in X-ray powder patterns of $Li_7[VN_4]$ samples obtained above 1070 K reflections not allowed in the space group $P\bar{4}3n$. Recently, we have obtained single crystals $Li_7[VN_4]$ from Li melt at 1173 K.[16] The single-crystal structure refinement supported our suspicion of a polymorph in the $Li_7[TaN_4]$ structure type with the space group $Pa\bar{3}$. These facts and the interesting thermal decomposition behavior of $Li_7[MnN_4]$ and $Li_3[FeN_2]$ led us to investigate the thermal behavior of $Li_7[VN_4]$ above 900 K.

Experimental Section

Syntheses and Characterization. All manipulations were carried out under dry argon in a glovebox ($p(O_2,H_2O) < 0.1$ ppm). The reactions in nitrogen or argon atmosphere were carried out in tantalum or tungsten crucibles contained within steel tubes. This assembly was placed in a quartz tube with ambient back-pressure of the respective gas. Li_3N was prepared from elemental lithium (rods, Alfa, 99.9%) and nitrogen (Messer-Griesheim, 99.999%, additionally purified by passing over molsieve, Roth 3 Å, and BTS-catalyst, Merck) of ambient pressure at 670 K. VN was obtained from VCl_3 (Alfa 99.9%) in flowing ammonia (Messer-Griesheim 99.998%) at 973 K. Single-phase samples of lithium nitridovanadates can be obtained from Li_3N, VN, and nitrogen of ambient pressure at temperatures above 920 K.

Cubic γ-$Li_7[VN_4]$ was obtained at 920 K (30 h) or 1020 K (10 h) in N_2 atmosphere as a yellow-grayish powder (chemical analyses: Li, 29.2 ± 0.7 wt %; V, 31.0 ± 1.0 wt %; i.e., $Li_{6.9}VN_4$). Annealing for a longer time (1020 K, 50 h) or at higher temperatures (1070 °C, 20 h) provides β-$Li_7[VN_4]$. In some patterns both phases were observed. Annealing of such mixtures γ-$Li_7[VN_4]$/β-$Li_7[VN_4]$ at 970 K, 50 h did not lead to γ or β single-phase material. Thus, the phase transition at this temperature is very slow in this temperature range.

Single-phase cubic β-$Li_7[VN_4]$ was synthesized from the binary nitrides at longer annealing times and/or higher temperatures (1020−1120 K, 20−50 h, N_2) as a yellow powder (chemical analyses: Li, 29.6 ± 0.3 wt %; V, 31.6 ± 0.3 wt %; i.e., $Li_{6.9}VN_4$).

Tetragonal α-$Li_7[VN_4]$ was obtained in a N_2 atmosphere in two ways: (i) at the same conditions as for cubic β-$Li_7[VN_4]$ (1020 K, 20 h, then 1120 K, 2 h), but in a V foil envelope, or (ii) by heat treatment of cubic β-$Li_7[VN_4]$ (1370 K, 5h). The second way provides a Li-deficient product; thus, a homogeneity region of this phase must be supposed. Yellow samples prepared by route i have the tetragonal unit cell parameters $a = 675.90(2)$ pm, $c = 488.34(2)$ pm, $V = 223.09(1) \times 10^6$ pm^3 and a molar ratio n(Li)/n(V) = 7.2 according to chemical analysis (Li, 30.6 ± 0.2 wt %; V, 31.4 ± 0.2 wt %; N, 32.69 ± 0.01 wt %; O, not detected < 0.10 wt %; i.e., $Li_{7.2}VN_{3.8}$). The unit cell of yellow-greenish samples prepared on route ii is slightly smaller: $a = 675.51(2)$ pm, $c = 488.05(3)$ pm, $V = 222.70(1) \times 10^6$ pm^3, n(Li)/n(V) = 6.5 (Li, 29.5 ± 0.2 wt %; V, 33.2 ± 0.2 wt %; i.e., $Li_{6.5}VN_{4-x}$). This lithium content is in agreement with the observed mass loss after heating supposing loss of Li_3N. The powder diffraction patterns presented were taken on a sample prepared in way i. The necessary large amount of sample (about 2 g) for the neutron diffraction contained a small amount of the β-polymorph as observed in the X-ray diffraction pattern. In the presence of liquid Li at 1270 K, 1 h,

Table 1. Profile Refinement Parameters for γ-, β-, and α-$Li_7[VN_4]$ (X-ray Data/Neutron Data)

phase	γ-$Li_7[VN_4]$	β-$Li_7[VN_4]$	α-$Li_7[VN_4]$
space group, Z	$P\bar{4}3n$, No. 218, 8	$Pa\bar{3}$, No. 205, 8	$P4_2/nmc$, No. 137, 2
a [pm], Guinier	960.90(4)	959.48(3)	675.90(2)
c [pm]			488.34(2)
V [10^6 pm^3]	887.23(6)	883.31(5)	223.09(9)
a [pm], Rietveld	960.64(1)	958.59(1)	675.75(1)
c [pm]			488.18(1)
radiation [pm]	Cu Kα_1	Cu Kα_1	Cu Kα_1/179.885
2θ range [deg]	15−100	13−100	12−88/10−160
step size [deg]	0.005	0.005	0.005/0.1
no. of params refined	30	32	39
structural params	14	16	11
χ^2	3.59	0.41	0.98/1.06
reliability value R_p	0.023	0.030	0.034/0.058

Table 2. Positional and Isotropic Displacement Parameters for γ-$Li_7[VN_4]$

atom	site	x	y	z	B [Å^2]
V(1)	2*a*	0	0	0	3.06(6)
V(2)	6*c*	1/4	1/2	0	3.51(4)
N(1)	8*e*	0.3907(4)	x	x	1.28(5)
N(2)	24*i*	0.1150(3)	0.1384(2)	0.3959(5)	B(N(1))
Li(1)	12*f*	0.257(6)	1/2	1/2	3.7(1)
Li(2)	6*d*	1/4	0	1/2	B(Li(1))
Li(3)	6*b*	0	0	1/2	B(Li(1))
Li(4)	8*e*	0.255(2)	x	x	B(Li(1))
Li(5)	24*i*	0.028(2)	0.244(3)	0.243(3)	B(Li(1))

Table 3. Positional and Isotropic Displacement Parameters for β-$Li_7[VN_4]$

atom	site	x	y	z	B [Å^2]
V(1)	8*c*	0.3703(2)	x	x	2.53(3)
N(1)	8*c*	0.2610(6)	x	x	1.30(4)
N(2)	24*d*	0.4858(5)	0.2575(3)	0.4786(2)	B(N(1))
Li(1)	8*c*	0.125(2)	x	x	1.76(9)
Li(2)	24*d*	0.132(1)	0.383(1)	0.136(2)	B(Li(1))
Li(3)	24*d*	0.357(1)	0.379(1)	0.1141(9)	B(Li(1))

Table 4. Positional and Isotropic Displacement Parameters for α-$Li_7[VN_4]$

atom	site	x	y	z	B [Å^2]
V	2*a*	3/4	1/4	3/4	0.89(5)
N	8*g*	3/4	0.4761(2)	0.5383(3)	0.54(3)
Li(1)	8*f*	0.9867(6)	$-x$	1/4	0.5(1)
Li(2)	4*d*	3/4	3/4	0.838(2)	1.6(2)
Li(3)	2*b*	1/4	3/4	3/4	1.3(1)

Table 5. Selected Distances in α-$Li_7[VN_4]$

V−N	184.4(1)	4×	Li(2)−N	235.9(6)	2×
V−Li ≥	251.6(4)			209.4(5)	2×
Li(1)−N	207.3(4)	2×	Li(3)−N	207.71(9)	4×
	213.2(3)	2×			

(17) Schnick, W.; Lücke, J. *J. Solid State Chem.* **1990**, *87*, 101.
(18) Vennos, D. A.; DiSalvo, F. J. *Acta Crystallogr. C* **1992**, *48*, 610.
(19) Wachsmann, Ch.; Jacobs, H. *J. Alloys Compd.* **1992**, *190*, 113.

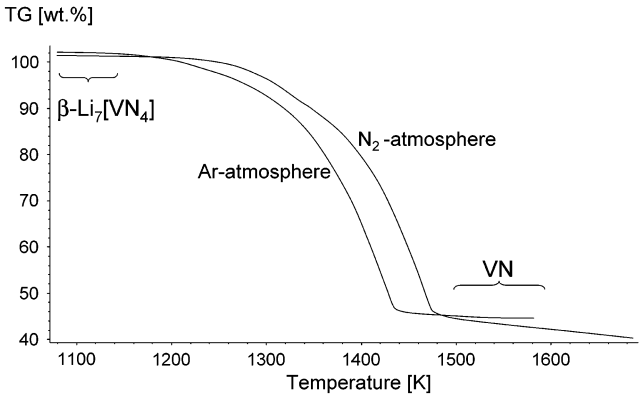

Figure 1. Thermogravimetric measurement of the decomposition of $Li_7[VN_4]$ in Ar and N_2 atmosphere (heating rate 1 K/min, starting phase β-$Li_7[VN_4]$).

α-$Li_7[VN_4]$ and γ-$Li_7[VN_4]$ convert into β-$Li_7[VN_4]$, a fact that might be connected with the homogeneity range of α-$Li_7[VN_4]$ addressed above. At temperatures above 1270 K in open crucibles under Ar or N_2 atmosphere $Li_7[VN_4]$ increasingly decomposes under release of Li_3N and N_2 as indicated in DTA/TG measurements (Figure 1). The final decomposition product at 1670 K is VN if a heating rate of 1 K/min is applied. With faster heating rates the decomposition shifts to considerably higher temperatures. Though there are no well-defined steps in the TG curve, X-ray diffraction patterns of samples quenched from various maximum temperatures indicate several more phases in the thermal decomposition of α-$Li_7[VN_4]$ to VN.

Solid solutions were obtained from γ-, β-, or α-phase samples and Li_2O at 1070−1170 K in nitrogen atmosphere up to 20 wt % of oxygen.

Chemical Analyses. Chemical analyses were carried out using the hot-extraction technique on a LECO analyzer TC-463 DR. The typical oxygen content in the ternary nitride samples was 0.2 wt %, with its origin mainly from an oxide impurity of 0.3 wt % in the VN starting material. Quantitative analyses of Li and V were performed using an ICP-OES (Varian Vista RL). All values are averages of at least 3 independent measurements.

Crystal Structure Determination and Refinements. The binary and ternary nitrides were characterized by X-ray powder diffraction using an imaging plate Guinier camera (HUBER diffraction, Cu $K\alpha_1$ radiation, 4×15 min scans, $8° \leq 2\Theta \leq 100°$). In each case, the sample was loaded between two polyimide foils in an aluminum cell with a rubber seal to exclude any moisture. Comparison of the powder patterns of the first and the final scan did not indicate any significant hydrolysis during the measurement procedure.

Neutron diffraction data on a microcrystalline sample of α-$Li_7[VN_4]$ were gathered at the E9 powder diffractometer at BERII, HMI Berlin, Germany. The sample was contained in a gastight vanadium cylinder (diameter 6 mm, length 51 mm, wall thickness 0.15 mm). For Rietveld refinements of γ- and β-$Li_7[VN_4]$ based on X-ray diffraction data the positional parameters of $Li_7[MnN_4]$ ($P\bar{4}3n$)[12] and $Li_7[VN_4]$ ($Pa\bar{3}$)[16] obtained from single crystals were used as initial parameters, respectively. For α-$Li_7[VN_4]$ the positional parameters of $Li_6\square[MoN_4]$[14] were used, and the unoccupied tetrahedral hole was filled with an additional Li site leading to the given composition. The structure was refined simultaneously against both patterns. Figures 2−4 depict the experimental diffraction patterns together with the calculated profiles and the difference curves of the observed and the simulated patterns as determined by least-squares refinements (Tables 1−5, program package FULLPROF[20]).

Magnetic Susceptibility. Measurements of the magnetization were carried out in a SQUID magnetometer (MPMS XL-7, Quantum Design) between 1.8 and 400 K at different magnetic fields. Corrections for the sample containers were applied. Since the diamagnetic increment of N^{3-} is only poorly established, we did not correct for the core-diamagnetism.

Thermal Analyses. DTA/TG measurements were performed on a STA 449C (Ar or N_2 atmosphere purified as described above, Ni crucibles, thermocouple type S, NETZSCH Gerätebau, Selb, Germany) completely integrated into a glovebox to avoid any hydrolysis. Temperature calibration was obtained using 5 melting standards in the temperature range of 370 and 1470 K.

X-ray Spectroscopy. For the XAS measurements powder samples were mixed with 3 times their volume of dried B_4C to produce homogeneous absorbers. Air-sensitive samples were loaded in steel capsules, equipped with Be windows (0.5 mm). Due to the extreme moisture sensitivity and the necessary way of handling of these samples, thickness effects in the resulting XAS spectra are inevitable.[29,30] Nonsensitive samples (V oxides) were prepared on Mylar film. The V K-edge measurements were performed in transition geometry at the E4 bending magnet beamline located at the DORISIII storage ring in the HASYLAB laboratory (DESY Hamburg, Germany). The X-ray beam outgoing from the bending magnet and formed with the toroidal and plane golden mirrors was monochromized using a double crystal monochromator, equipped with a Si(111) crystal. The absorption spectra of the vanadium compounds were measured simultaneously with the spectrum of metallic vanadium foil serving as a reference for energy calibration.

Results and Discussion

$Li_7[VN_4]$ forms from Li_3N and VN in nitrogen atmosphere above 920 K. Depending on the preparation conditions three polymorphs are obtained and characterized. As indicated by DTA measurements (no signal detected) the transformations between these phases are slow. As shown by thermogravimetric measurements at temperatures above 1270 K (1070 K at longer annealing times, open crucibles, see Experimental Section) decomposition starts, finally leading to VN (Figure 1).

The crystal structure of γ-$Li_7[VN_4]$ was originally reported by Juza for this composition and for $Li_7[MnN_4]$;[10] $Li_7[PN_4]$ is an isotype.[17] Single crystals of β-$Li_7[VN_4]$ can be obtained

(20) (a) Roisnel, T.; Rodriguez-Carvajal, J. *WinPLOTR*, version May 2000; Materials Science Forum, Proceedings of the Seventh European Powder Diffraction Conference 2000, Barcelona, Spain, p 118. (b) Rodriguez-Carvajal, R. *FULLPROF.2k*, version 1.6; Laboratoire Léon Brillouin: 2000. In Abstract of Satellite Meeting on Powder Diffraction, Congress of the International Union of Crystallography, Toulouse, France 1990, p 127.
(21) Bärnighausen, H. *MATCH, Commun. Math. Chem.* **1980**, *9*, 139.
(22) Juza, R.; Uphoff, W.; Gieren, W. *Z. Anorg. Allg. Chem.* **1957**, *292*, 71.
(23) Grunes, L. A. *Phys. Rev. B* **1983**, *27*, 2111.
(24) de Groot, F. M. F. *J. Electron. Spectrosc. Relat. Phenom.* **1994**, *67*, 529.
(25) Shulman, R. G.; Yafet, Y.; Eisenberger, P.; Blumberg, W. E. *Proc. Natl. Acad. Sci. U.S.A.* **1976**, *73*, 1384.
(26) E.g.: Durrant, P. J.; Durrant, B. *Introduction to Advanced Inorganic Chemistry*, 2nd ed.; Longman Group: London, 1970; p 976.
(27) Leapman, R. D.; Grunes, L. A. *Phys. Rev. Lett.* **1980**, *45*, 397.
(28) Leapman, R. D.; Grunes, L. A.; Fejes, P. L. *Phys. Rev. B* **1982**, *26*, 614.
(29) Pease, D. M. *Appl. Spectrosc.* **1976**, *30*, 405.
(30) Szmulowicz, F.; Pease, D. M. *Phys. Rev. B* **1978**, *17*, 3341.

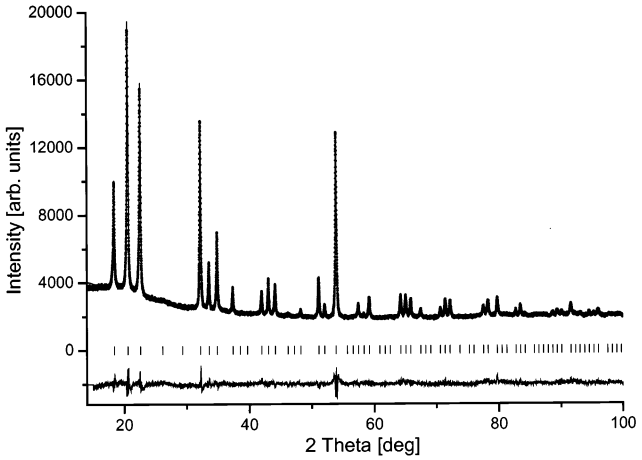

Figure 2. X-ray powder diffraction diagram of γ-$Li_7[VN_4]$ (Cu Kα_1 radiation). The measured data are shown as points, the continuous line represents the calculated profile, and the lower line shows the difference between the calculated and observed intensities. The marks below the data indicate the positions of the reflections.

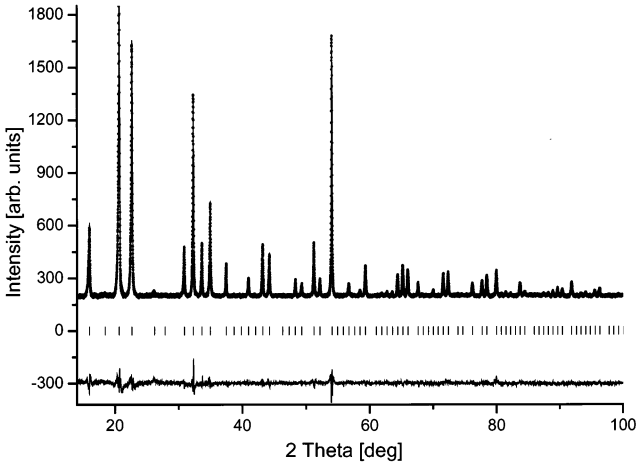

Figure 3. X-ray powder diffraction diagram of β-$Li_7[VN_4]$ (Cu Kα_1 radiation). The measured data are shown as points, the continuous line represents the calculated profile, and the lower line shows the difference between the calculated and observed intensities. The marks below the data indicate the positions of the reflections.

in the presence of elemental lithium.[16] The latter fact corresponds to our observation that in liquid Li at 1270 K both α- and γ-$Li_7[VN_4]$ transform into β-$Li_7[VN_4]$. The light yellow color of all lithium nitridovanadates indicates the oxidation state of +5 for vanadium, corresponding to the compositions from structure refinements and to the results from XAS spectroscopy (see below). Measurements of the magnetic susceptibility reveal diamagnetic behavior.

The crystal structures of γ-, β-, and α-$Li_7[VN_4]$ are depicted in Figure 5. A comparison reveals that all three structures are based on Li_2O superstructures with nitrogen on the oxygen site and an ordered distribution of Li and V on the lithium position. γ- and β-$Li_7[VN_4]$ crystallize in cubic $2 \times 2 \times 2$ supercells with 8 formula units in the crystallographic unit cell. The unit cell of α-$Li_7[VN_4]$ is tetragonal. The three polymorphs differ in the ordering scheme of Li and V atoms within a fcc arrangement of nitrogen. As a general rule $[VN_4]^{7-}$ tetrahedra are always isolated, i.e., they do not share corners or edges. The volume per formula unit

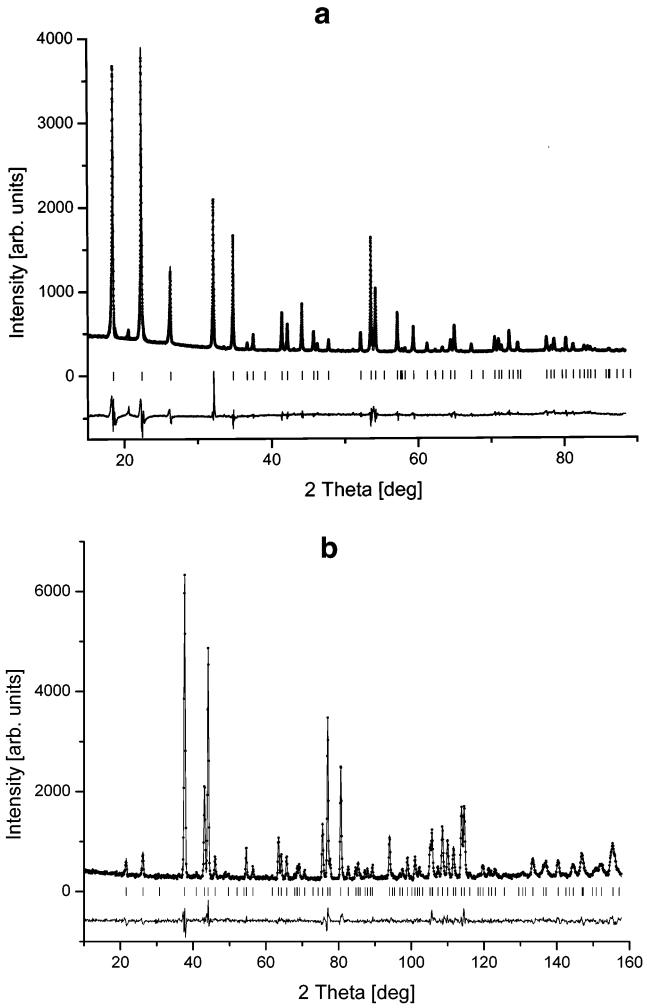

Figure 4. (a) X-ray (Cu Kα_1 radiation) and (b) neutron (λ = 179.885 pm) powder diffraction diagrams of α-$Li_7[VN_4]$. The measured data are shown as points, the continuous line represents the calculated profile, and the lower line shows the difference between the calculated and observed intensities. The marks below the data indicate the positions of the reflections.

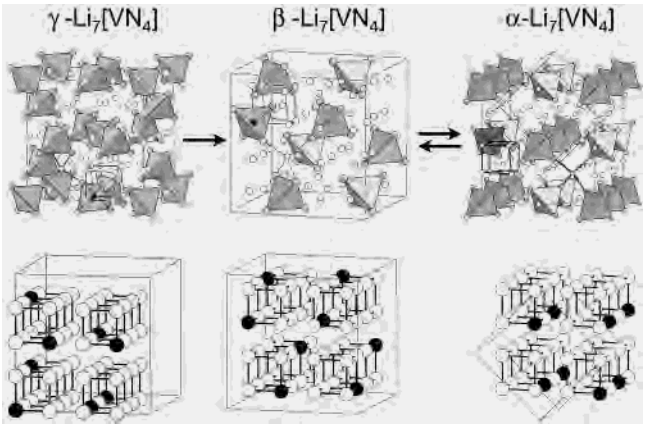

Figure 5. Comparison of the crystal structures of γ-$Li_7[VN_4]$ (left), β-$Li_7[VN_4]$ (middle), and α-$Li_7[VN_4]$ (right). Top: The arrangement of isolated $[VN_4]^{7-}$ tetrahedra differs within the ordered Li_2O-type superstructures. Below: Idealized sections of the crystal structures of γ-$Li_7[VN_4]$ (left), β-$Li_7[VN_4]$ (middle), and α-$Li_7[VN_4]$ (right). Black spheres represent V, and open spheres represent Li. Nitrogen atoms are omitted for clarity.

of γ-$Li_7[VN_4]$ with $V(\gamma) = 110.90(1) \times 10^6$ pm^3 is slightly larger than that of β-$Li_7[VN_4]$, $V(\beta) = 110.41(1) \times 10^6$ pm^3.

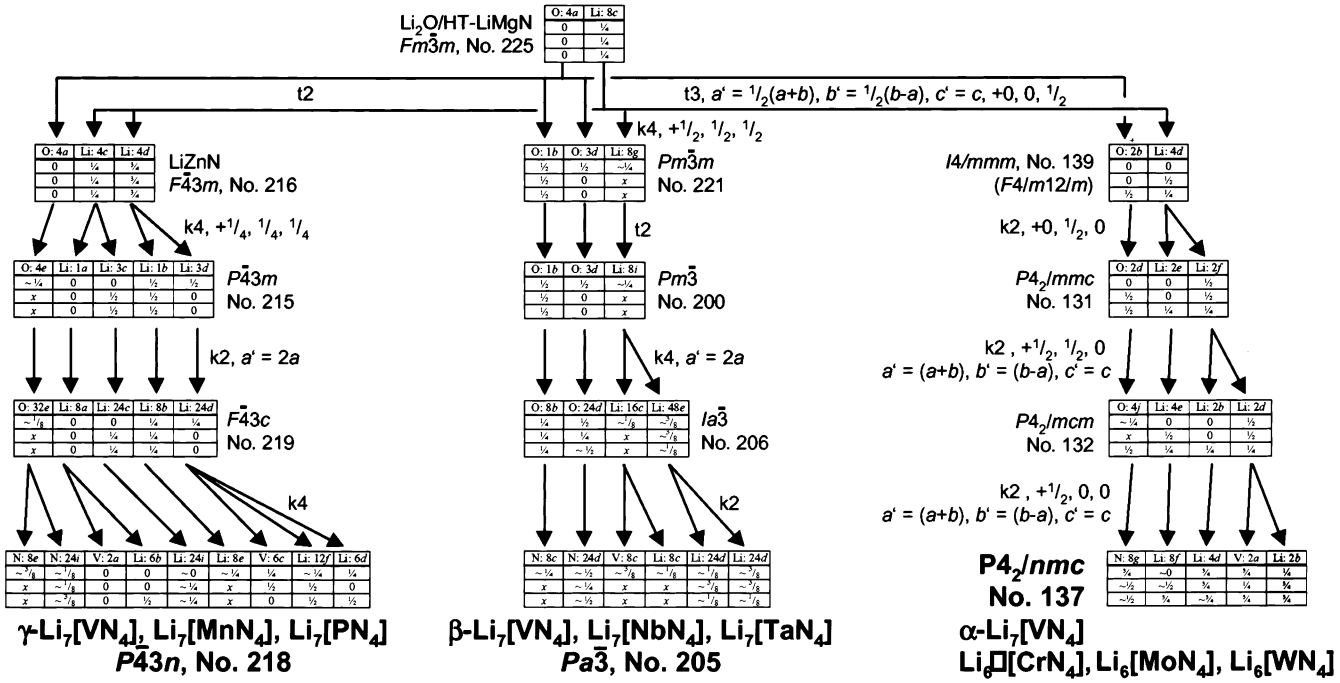

Figure 6. "Bärnighausen" symmetry tree, that relates the three polymorphs of $Li_7[VN_4]$ to Li_2O. Note that no direct group−subgroup relations between the polymorphs exist. The shaded site for α-$Li_7[VN_4]$ indicates the empty position in the compounds $Li_6[MN_4]$ (M = Cr, Mo, W).[14]

Single-phase γ-$Li_7[VN_4]$ is obtained at lower temperatures (920−970 K) than used for β-$Li_7[VN_4]$, or at shorter reaction times at 1020−1070 K. With longer annealing times or at somewhat higher temperatures always β-$Li_7[VN_4]$ was observed in the product, either single phase or with admixtures of γ-$Li_7[VN_4]$ or α-$Li_7[VN_4]$ depending on the conditions. Thus, we argue that γ-$Li_7[VN_4]$ is metastable, first formed in the reaction of Li_3N with VN under nitrogen atmosphere. At higher temperatures or longer annealing times the phase is rearranged to β-$Li_7[VN_4]$ according to the Ostwald rule. Above 900−1000 K β-$Li_7[VN_4]$ transforms to α-$Li_7[VN_4]$ with a larger volume per formula unit of $V(\alpha) = 111.55(1) \times 10^6$ pm^3, as expected for a high-temperature phase.

The crystal structure of α-$Li_7[VN_4]$ is closely related to those of $Li_6[MoN_4]$ and $Li_6[WN_4]$ (and probably $Li_6[CrN_4]$).[14] The unit cell dimensions are comparable: α-$Li_7[VN_4]$, a = 675.90(2) pm, c = 488.34(8) pm; $Li_6[CrN_4]$, a = 673.4(2) pm, c = 483.3(2) pm; $Li_6[MoN_4]$, a = 667.3(1) pm, c = 492.5(3) pm; $Li_6[WN_4]$, a = 667.9(1) pm, c = 492.7(1) pm. The crystal structures of $Li_6[MoN_4]$ and $Li_6[WN_4]$ are also based on Li_2O superstructures and can be written according to $Li_6\square[MN_4]$ (□ denotes a vacancy in the metal substructure, M = Mo, W). The crystal structure of α-$Li_7[VN_4]$ simply relates by filling the vacancy in the $Li_6\square[MN_4]$ structures with one additional lithium per formula unit.

Distances d(V−N) range from 181.4(6) pm to 186.4(4) pm in the three polymorphs. Distances d(V(1)−N(1)) = 181.8(4) pm and d(V(2)−N(2)) = 183.6(3) pm for the two crystallographic inequivalent $[VN_4]^{7-}$ tetrahedra in γ-$Li_7[VN_4]$ are slightly longer than in the isotypic $Li_7[MnN_4]$ (181.4(1) pm, 182.6(3) pm[12]) as may be expected from ionic radii considerations. Similarly, the structural data obtained for β-$Li_7[VN_4]$ (d(V−N(1)) = 181.4(6) pm, 1×, d(V−N(2)) = 186.4(4) pm, 3×) agree with the data previously obtained from single-crystal refinements (d(V−N(1)) = 181.3(6) pm, 1×, d(V−N(2)) = 185.1(3) pm, 3×[16]). On average these distances are larger than those of the γ-phase, despite the larger unit cell of the low-temperature polymorph. The average distances $\bar{d}$(Li−N) = 213 and 211 pm in γ- and β-$Li_7[VN_4]$, respectively, are in the range expected for lithium in tetrahedral coordination by nitrogen, but due to the large uncertainties in the positional parameters of Li from X-ray powder diffraction the differences are not significant, and, thus, we are not going to discuss these distances in deeper detail. In α-$Li_7[VN_4]$ the distance d(V−N) = 184.4(1) pm and the range of distances d(Li−N) = 207.3(4)−235.9(6) pm are much more reliable, since they were obtained from combined X-ray and neutron diffraction data. This combination is essential for the structure solution and refinement from powder, because the neutron scattering length of V is close to zero, while the contribution of Li to the X-ray diffraction pattern is small. Especially, the special position Li(3) (d(Li−N) = 207.7(1) pm, 4×) should be mentioned, since this position is not occupied in the group 6 compounds $Li_6[MoN_4]$ and $Li_6[WN_4]$ as required by charge balance.

Figure 6 resembles a "Bärnighausen" symmetry tree[21] for the crystal structures of the polymorphs of $Li_7[VN_4]$. It should be noted that there is no direct group−subgroup relation between any of the structures of the polymorphs. Since the first coordination sphere of all atoms is basically identical (Li, V, tetrahedral by 4 N; N, cubic by 7 Li + 1 V) the phase transitions must be reconstructive with changes only in higher coordination spheres according to the classification of Buerger.[32] Figure 5 (bottom) compares the metal atom

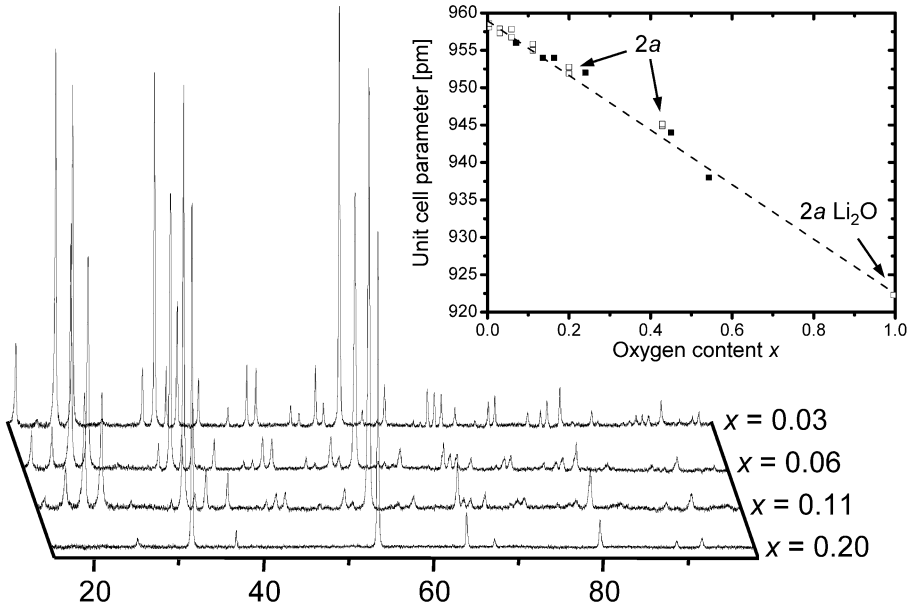

Figure 7. X-ray diffraction patterns of solid solution phases of the general formula $Li_{1.75}\{(V_{0.25(1-x)}Li_{0.25x})(N_{1-x}O_x)\}$ with $x = 0.20$ (front, a small unknown impurity phase can be seen in this pattern), $x = 0.11$ (second), $x = 0.06$ (third), and $x = 0.03$ (last). Inset: Unit cell parameters of the solid solution series as a function of the oxygen content x and extrapolation to (two times) the unit cell of Li_2O (open symbols, this study; solid symbols, data taken from the literature[22]).

arrangements in the three structures. As can be seen the vanadium and lithium atoms are arranged together in a primitive cubic array (within tetrahedral coordination by nitrogen, which is omitted for clarity). The only difference is the relative arrangement of these metal ions governing the symmetry of the structure. The unusual decrease in symmetry from cubic to tetragonal at the high-temperature transformation is attributed to the smaller primitive unit cell volume of the tetragonal unit cell following the tendency of a decreasing number of occupied sites with increasing temperature (from γ-, β-, to the α-polymorph).

We additionally studied the solid solution series of $Li_7[VN_4]$ with Li_2O with the general formula $Li_{1.75}\{(V_{0.25(1-x)}Li_{0.25x})(N_{1-x}O_x)\}$ and $0 \leq x \leq 1$, that was earlier observed by Juza et al.[22] With increasing oxygen content the unit cell parameter of the product decreases linearly. An extrapolation to the oxygen content of Li_2O indicates that the volume changes of the solid solution series are in accordance with Vegard's law for the full range of compositions (Figure 7). Rietveld refinements on the X-ray patterns suggest an exchange of V by Li and simultaneously only very small occupation of the Li sites by V ($\leq$3%) within the structural model of β-$Li_7[VN_4]$. Total disorder is reached at a composition near $x = 0.125$ as is indicated in powder X-ray diffraction patterns: reflections demanding the superstructure cell of $a \approx 1000$ pm disappear, leading to $a' \approx {}^1/_2a \approx 500$ pm (Figure 7). This composition ($x = 0.125$) corresponds to the replacement of one $[VN_4]^{7-}$ tetrahedron per cubic unit cell, i.e., one formula unit $Li_7[VN_4]$ by 4 Li_2O per unit cell. Since the samples were prepared at 1070−1170 K, we never observed a solid solution in the structure of the α-$Li_7[VN_4]$ polymorph, but addition of small amounts of oxygen ($\approx$2 wt %) turn the α-phase to the cubic solid solution phase.

XAS spectroscopy at the absorption thresholds is an element specific tool, that can provide valuable information on the oxidation state and the electronic configuration of most atomic components of both crystalline and amorphous materials. The shape and energy position of the absorption spectrum in its near-edge region is closely related to the electronic structure, partly also influenced by the magnetic state, the local symmetry, and the coordination environment of the nuclei, while the oscillation observed in the high-energy region of the spectrum is associated with the arrangement of the atoms, i.e., the local surroundings. Due to these features XAS spectroscopy today is widely used in physics and materials sciences, but in chemistry it is still not well established.

In V−K XAS spectra a V 1s core−electron is exited to the related 4p states setting on the continuum according to dipole selection rules. In general XAS spectra of the first-row transition metals have a weak preedge structure about 10 eV below the absorption edge. This feature was assigned as originating from a 1s−3d transition.[23−25] For compounds with the transition metal in a centrosymmetric environment, a 1s−3d transition is electric dipole forbidden by parity considerations. (The fact that dipole selection rules hold only in systems with an inversion center is known in spectroscopy as Laporte's rule.[26]) However, a weak preedge feature is still experimentally observed. In the case of non-centrosymmetric local surroundings the V-4p states are strongly mixed with 3d orbitals; therefore the spectral weight of 3d states can be enhanced. All this may lead to a significant preedge feature that is more intense for local symmetries lacking an inversion center. In particular, the features in the region of the 1s−3d

(31) Hu, Z.; Kaindl, G.; Meyer, G. *J. Alloys Compd.* **1997**, *246*, 186.
(32) Buerger, M. J. *Fortschr. Miner.* **1961**, *39*, 9. Buerger, M. J. In *Phase Transformations in Solids*; Smoluchowski, R., Mayer, J. E., Weyl W. E., Eds.; John Wiley: New York, 1951.

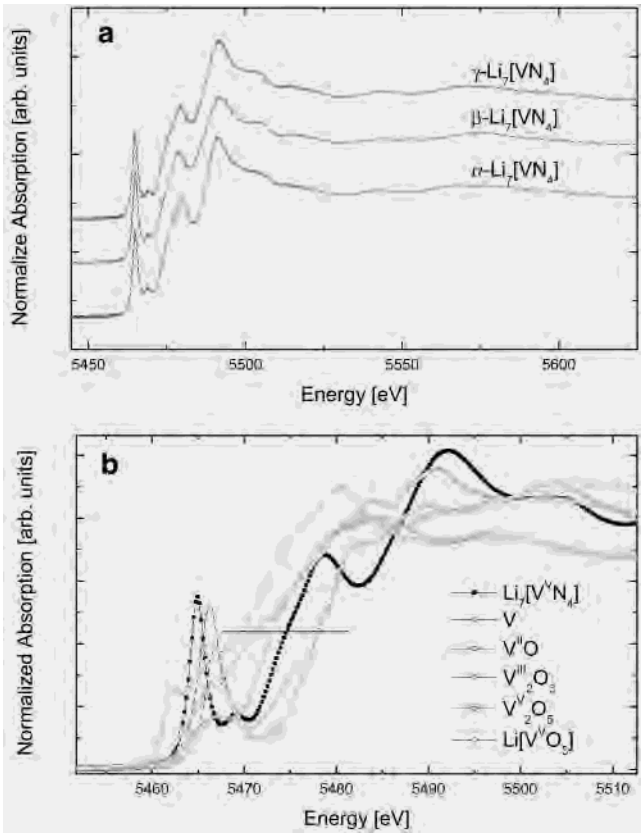

Figure 8. (a) XAS spectra at the V K-edge of α-, *β*-, and *γ*-$Li_7[VN_4]$ and (b) comparison to the spectra of V, $V^{II}O$, $V^{III}{}_2O_3$, $V^{V}{}_2O_5$, and $Li[V^{V}O_3]$.

transition have been shown to be sensitive to the oxidation state and geometry of a 3d transition metal atom.[25]

X-ray absorption probes the unoccupied part of the electronic structure of the system. Thus, for all following discussions it should be mentioned that from exited states with a V 1s hole information on the ground state is derived, therefore the conclusions might not be uncritical. We chose to measure K-edge spectra, because (i) the relevant energies make it possible to work in transition mode, hence to use fully encapsulated samples (necessary for strongly air sensitive compounds), and (ii) the valence state can directly be taken from the energy shift of the main absorption edge, while in $L_{2,3}$ XAS spectra the edge of oxidized 3d metals can lie at higher or lower energies than these of the corresponding elemental metal. The latter fact is due to strong multiplet interactions in the final state effects.[27,28]

Figure 8a compares the vanadium K-edge XAS spectra of *γ*-, *β*-, and α-$Li_7[VN_4]$. As can clearly be seen there is nearly no difference in prepeak and edge energy position and shape. This indicates an identical oxidation state and local symmetry of the vanadium atoms coordinated by nitrogen ligands. At higher energies the EXAFS region starts, which features are connected mostly with the first and second coordination sphere of the absorbing atom. Since the coordination spheres surrounding V in all three polymorphs are very similar, this region is also basically identical in all three spectra.

Figure 8b gives a comparison of the vanadium K-edge XAS spectra of *γ*-, *β*-, and α-$Li_7[VN_4]$ with vanadium metal and several vanadium oxides. The most prominent feature is the strong and well-separated preedge feature (at around 5467 eV) of the ternary nitrides and the vanadium(V) oxides $V^{V}{}_2O_5$ and $Li[V^{V}O_3]$. As mentioned above this preedge is due to an electric dipole forbidden 1s−3d transition. The occurrence of a strong preedge feature is a clear indication for non-centrosymmetric first coordination sphere of the absorbing atom in V_2O_5 (1 + 3 + 1 coordination), $Li[VO_3]$ (tetrahedral coordination), and the discussed ternary nitridovanadates. The absorption edges selected at about 0.6 of the edge jump shift from metallic vanadium over $V^{II}O$ and $V^{III}{}_2O_3$ to $V^{V}{}_2O_5$ and $Li[V^{V}O_3]$ to higher energies indicating the higher oxidation state of vanadium. The edges of the three polymorphs of $Li_7[V^{V}N_4]$ fit nicely in between $V^{III}{}_2O_3$ and $V^{V}{}_2O_5$/$Li[V^{V}O_3]$. This is easily understood from the smaller electronegativity of the nitrogen ligands compared to oxygen. As observed earlier the absorption edge is shifted to higher energies with increasing electronegativity of the ligands.[31] The preedge peak in the three polymorphs of $Li_7[V^{V}N_4]$ is much narrower than those in the vanadium oxides indicating strongly localized 3d orbitals due to the isolated $[VN_4]^{7-}$ nitridometalate ions. This results in 3d related states well separated from the main absorption edge. In this case the main-edge shift is more reliable than the preedge shift to determine the metal ion valence.

As conclusion one should note that apparently in many nitride systems the structures reported so far probably are only the most stable compound or phase, mostly obtained by chance as single crystals. A similar rich phase diagram as previously demonstrated for the Li−Mn−N system[12] and shown in the present work for Li−V−N can be anticipated for many nitridometalate systems.

Acknowledgment. We thank U. Schmidt and B. Bayer for performing the chemical analyses, Dr. Yu. Prots' and Dr. R. Cardoso for collecting the X-ray diffraction data, Dr. W. Schnelle for the measurements of the magnetic susceptibilities, and Prof. Dr. R. Kniep for his constant interest and support. We also wish to thank Prof. U. Müller for a discussion of the symmetry relations. The neutron diffraction pattern was taken by Dr. G. Auffermann at the E9 diffractometer operated by Dr. D. Többens. We would also like to acknowledge the help of Dr. K. Klementiev at beamline E4 (Hasylab at Desy).

Supporting Information Available: Rietveld refinement details. This material is available free of charge via the Internet at http://pubs.acs.org.

IC020653B